Dental Materials 40 (2024) 1199–1207

Contents lists available at ScienceDirect

Dental Materials

journal homepage: www.elsevier.com/locate/dental

Full length article

Ceramic conversion treated titanium implant abutments with gold for enhanced antimicrobial activity

Yasser M. Aly [a,b], Zhenxue Zhang [c], Nesma Ali [b], Michael R Milward [b], Gowsihan Poologasundarampillai [b], Hanshan Dong [c], Sarah A. Kuehne [d], Josette Camilleri [b,*]

[a] Faculty of Dentistry, Alexandria University, Alexandria, Egypt
[b] School of Dentistry, Institute of Clinical Sciences, College of Medical and Dental Sciences, University of Birmingham, Birmingham, United Kingdom
[c] School of Metallurgy and Materials, College of Engineering, University of Birmingham, Birmingham, United Kingdom
[d] School of Science & Technology, Nottingham Trent University, Nottingham, United Kingdom

ARTICLE INFO

Keywords:
Titanium
Implant abutments
Antimicrobial properties
Gold
Ceramic conversion treatment

ABSTRACT

Introduction: Peri-implantitis is an inflammatory process around dental implants that is characterised by bone loss that may jeopardize the long-term survival of osseo integrated dental implants. The aim of this study was to create a surface coating on titanium abutments that possesses cellular adhesion and anti-microbial properties as a post-implant placement strategy for patients at risk of peri-implantitis.

Materials and Methodsmethods: Titanium alloy Grade V stubs were coated with gold particles and then subjected to ceramic conversion treatment (CCT) at 620 °C for 3, 8 and 80 h. The surface characteristics and chemistry were assessed using scanning electron microscopy (SEM), energy dispersive spectroscopy (EDS), and X-ray diffraction (XRD) analysis. The leaching profile was investigated by inductively coupled plasma mass spectroscopy (ICP-MS) for all groups after 7, 14 and 28 days in contact with distilled water. A scratch test was conducted to assess the adhesion of the gold coating to the underlying titanium discs. Two bacterial species (*Staphylococcus aureus (SA) & Fusobacterium nucleatum (FN)*) were used to assess the antibacterial behaviour of the coated discs using a direct attachment assay test. The potential changes in surface chemistry by the bacterial species were investigated by grazing angle XRD.

Results: The gold pre-coated titanium discs exhibited good stability of the coating especially after immersion in distilled water and after bacterial colonisation as evident by XRD analysis. Good surface adhesion of the coating was demonstrated for gold treated discs after scratch test analysis, especially titanium, following a 3-hour (3 H) ceramic conversion treatment. All coated discs exhibited significantly improved antimicrobial properties against both tested bacterial species compared to untreated titanium discs.

Conclusions: Ceramic conversion treated titanium with a pre-deposited gold layer showed improved antimicrobial properties against both SA and FN species than untreated Ti-C discs. Scratch test analysis showed good adherence properties of the coated discs the oxide layer formed is firmly adherent to the underlying titanium substrate, suggesting that this approach may have clinical efficacy for coating implant abutments.

1. Introduction

Tooth loss usually occurs due to periodontal disease, trauma, root canal treatment failures, and advanced non-restorable dental caries [1]. It has significant patient impact that affects the masticatory function, facial appearance, and aesthetics, which result in significant psychological and quality of life impacts [2]. To manage such challenges, the replacement of missing teeth is desirable.

One of the treatment modalities for tooth replacement is the use of dental implant supported prosthesis which is now considered the preferred treatment alternative for edentulous spaces. The use of osseointegrated implants was first reported in the 1980s, and thereafter studies shifted towards investigating the aesthetic requirements of implant restorations and extending their clinical applications from single tooth replacement to partial and complete replacement of teeth and management of orofacial defects [1,2].

* Correspondence to: School of Dentistry, 5, Mill Pool Way Edgbaston, Birmingham B5 7EG, United Kingdom.
E-mail address: J.Camilleri@bham.ac.uk (J. Camilleri).

https://doi.org/10.1016/j.dental.2024.05.029
Received 11 April 2024; Accepted 29 May 2024
Available online 8 June 2024

Dental implants have several advantages over conventional fixed prosthesis namely a decreased risk of caries and downstream endodontic problems of adjacent teeth. The success rate for dental implants nowadays exceeds 97 % with high levels of functional, biological, and esthetical satisfaction [3,4].

A typical titanium implant is composed of 3 components. The fixture which is threaded and is the main component embedded into bone; the abutment, which is placed on top of the fixture, over which the crown replacing the tooth is placed and is either cement or screw fixed. All components are made of either titanium or ceramic and the abutment and screw can be made of ceramic over a titanium fixture. Implants need careful monitoring for early identification of peri-mucositis and the potential for development of peri-implantitis which can ultimately lead to implant loss. Evaluation of radiographic bone loss around dental implants indicates various patterns of bone loss, depending upon jaw region, case type, bone quality, implant surface type, implant design, smoking status, and oral hygiene [5].

Despite the high success treatment rates, implant failures present due to initial gingival inflammation resulting from bacterial biofilm development (peri-mucositis) that can develop into peri-implantitis in susceptible individuals. A prevalence of 22 % [6,7] of peri-implant inflammation (periimplantitis) represents one of the most frequent complications in dental implantology affecting both the surrounding soft and hard tissues, which can lead to dental implant loss [6,8].

Long term maintenance of the implants is important as although initial osseointegration occurs, in the long-term dental implants may be lost due to peri-implantitis. Peri-implantitis is a multifactorial inflammatory disease, with the bacteria that grow on the abutment surface play a key role in its onset and exacerbation [9].

Abutment and restoration design are key factors in the development of peri-implantitis as they either provide desired properties for soft tissue healing and epithelial attachment or they may act as a factor initiating peri implant inflammation [10,11]. Other factors affecting the marginal bone level around dental implants include periodontal disease, diabetes, smoking, buccal soft tissue thickness, and implant stability [12]. Research on peri-implantitis highlights the need for long-term maintenance, and that the surface characteristics of the abutment offer considerable potential to minimize marginal bone loss [13].

Abutment modifications include zirconia coatings [14], ceramic conversion treated titanium with gold (Au) or silver (Ag) [15,16], modified polyetheretherketone [17], glasses containing nanoparticles and biofunctionalization with antibiotic-loaded coatings [18,19]. However, to date these modifications do not appear to offer improved clinical outcomes. Although antimicrobial nanomaterials are promising alternatives, their clinical use is challenging in terms of adequate dose delivery over a sufficient period to achieve the desired antimicrobial effect. Furthermore, the biocompatibility of these products is an important factor that is often excluded from the characterization of new materials. In addition, any toxic effects on the environment must be considered [20]. The aim of this study was to develop a modified coated abutment made of Grade V titanium aimed for patients who are susceptible to peri-implantitis as diabetic patients or hypertensive patients. It is envisaged that the coated abutment could be used as part of the follow-up care for patients who are at high risk of developing peri-implantitis.

2. Materials and methods

Prefabricated titanium alloy Grade V discs composed of Ti-6AL-4 V (L. Klein SA, Bienne, Switzerland) which were machined into discs 20 mm in diameter and 3.5 mm thick (Accura Tools, Playden, United Kingdom) were utilized for this study as it's the most used in the fabrication of titanium implants and abutments. They were ground progressively using 320, 600, 800 and 1200 grit Si-C discs (Struers, Ballerup, Denmark) using water coolant. All the discs were cleaned in an ultrasonic bath in the following sequence using acetone, 70 % alcohol and distilled water (20 min each).

Following the grinding and cleaning phase, heat treatment of the titanium surface was undertaken (Table 1). A thin layer (~20 nm) of gold (Au) was deposited on one side of the disc surface by sputter coating (Olympus Sputter Coaters, Evident, Southend-On-Sea, United Kingdom) at 25 mA for 5 min. Ceramic conversion treatments (CCT) were carried out in an electric furnace (Elite Thermal Systems Limited, Harborough, United Kingdom), with a ramp rate of 8 °C/min up to 620 °C. According to the CCT time, three groups of Au pre-coated discs and one control disc were used in this study (Table 1). This grouping was based on comparing the untreated titanium discs to Au CCT treated titanium discs at different heating times for surface properties, antimicrobial properties and adhesion of the surface coating formed using scratch testing.

2.1. Material characterization

Various characterization methods were used to assess the surface morphology, cross-sectional microstructure, and elemental and phase constituents of the ceramic conversion treated and control titanium alloy.

The scanning electron microscope (SEM: EVO MA10, Carl Zeiss, Cambridge, UK) equipped with an Oxford Inca energy dispersive X-ray spectroscopy (EDX) detector (Oxford Instruments, High Wycombe, United Kingdom) provided information on the surface microstructure and elemental analysis. To reveal the oxide layer characteristics, microstructure and thickness, discs were sectioned and mounted in conductive Bakelite and then smoothened by grit blast up to 4000 grit, followed by polishing using 9 μm diamond paste, and finished with activated colloidal silica. The polished discs were then etched in a Kroll's reagent of 2 % HF, 10 % HNO_3, and 88 % H_2O. After preparation, they were evaluated using SEM/EDX.

X-ray diffraction analysis was performed to assess the phases present in the surface. A diffractometer (Panalytical Empyrean X-ray Diffractometer), utilising a copper source (Kα – 1.54 Å) was used to identify the phase constituents on the surface of the samples. The X-ray patterns were acquired in the 2θ (20–70°) with a step of 0.02° and 0.6 s per step. Phase identification was established using a search-match software utilizing the ICDD database (International Centre for Diffraction Data, Newtown Square, PA, USA).

2.2. Assessment of coating adhesion

The adhesion strength of the oxide layers to the titanium disc was assessed by scratch tests using a ST30 Scratch Tester with a Rockwell spherical cone tip (Teer Coatings Ltd. Droitwich, England). The load increased gradually from 10 to 60 N with a linear velocity of 10 mm/min and loading rate of 100 N/ min. Formed scratches were then examined under the scanning electron microscope in secondary electron mode and 10k magnification to assess the coating's adherence and coherence.

2.3. Assessment of leaching

Ceramic conversion treated and control titanium discs were immersed in 5 ml distilled water in a sterile plastic container, and the

Table 1
Sample groups and the detailed ceramic conversion treatment parameters.

Specimen	Coating	Temperature °C	Heat treatment time hours	Oxide layer thickness mm
Ti-C	No coating	-	-	-
Au-Ti-3 H	Au	620	3	2.30 - 2.65
Au-Ti-8 H	Au	620	8	3.15 – 4.50
Au-Ti-80 H	Au	620	80	6.50 – 8.40

elemental leaching in solution was assessed by inductively coupled plasma mass spectroscopy (ICP-MS; Optima 8000, Perkin Elmer, Waltham, MA, USA) after 7, 14 and 28 days. Prior to testing, the leachate samples were acidified to a 2 % HNO_3 in a falcon tube and diluted 100-fold. A blank of distilled water was also included in the testing. The solution was changed after each measurement at 7days, 14 days and 28days. PH value for the solution was recorded using a pH meter (Fisherbrand™ accumet™ AB150 pH Benchtop Meters, Leicestershire, UK).

2.4. Antimicrobial properties

To assess the effectiveness of the new coating both aerobic and anaerobic bacteria which are dominant in the oral cavity and associated with peri-implantitis were selected in this study. Artificial gingival crevicular fluid (GCF) was prepared (60 % Roswell Park Memorial Institute (RPMI), 40 % horse serum, 0.5 ug/ml menadione and 5 ug/ml haemin). All the preparation steps were performed in a Class II ventilated hood to prevent contamination. The artificial GCF was used as a growth media for the tested bacterial species. The bacteria were grown overnight in an incubator at 37 °C. Two bacterial species, aerobic, Gram-positive *Staphylococcus aureus* (SA) ATCC23726 and anaerobic, Gram negative *Fusobacterium nucleatum* ssp, *nucleatum (FN)* FNN23 were used to assess the antimicrobial effect of the gold CCT specimens. For SA species, brain heart infusion (BHI) agar was used to grow bacterial colonies, and Schaedler Anaerobe Agar (SAA) for FN species. Three to four representative colonies were added to 5 ml GCF, and incubated overnight; for *SA*, in a shaking incubator at 37 °C for 24 h and for *FN* in an anaerobic chamber (Don Whitley, DG250, 10 %H, 10 % CO_2, 80 %N) at 37 °C for 24 h.

2.5. Direct attachment assay test

All work was carried out in a Class II ventilated hood for *SA* and in the anaerobic chamber for *FN*. The test titanium discs were sterilized by autoclaving at 121 °C, 15 Psi for 60 min. Four samples were run at a time: representing the four studied groups: blank untreated titanium discs (Ti-C) (positive control group), gold CCT discs (Au- Ti-3 H, Au-Ti-8 H, & Au-Ti-80 H). A filter paper was moistened with 600 µl sterile phosphate buffered saline (PBS; Sigma Aldrich UK) to maintain humidity. The test disc was placed onto a microscope slide with sterile forceps to avoid contamination. 1 ml of the overnight bacterial suspension was diluted in 9 ml of Brain Heart Infusion (BHI); 20 µl of this suspension was then pipetted onto titanium disc surface. A coverslip (2 cm x 2 cm) was carefully positioned on top to spread the inoculum over the entire disc surface area. The petri dishes were closed with lids, wrapped in cling film, labelled, and incubated at 37 °C, 5 % CO_2 for 24 h for *SA*. For *FN* the same procedure was completed but the petri dish was left in anaerobic chamber for 24 h.

Following the incubation period, the Ti disc and coverslip of each dish were transferred into 10 ml of (BHI). Each suspension was vortexed for 30 s at 1200 rpm (Fisher Scientific. Whirlmixer Cyclone Vortex Mixer CM-I, Loughborough, UK). Using a 96 well plate, (Sigma Aldrich., UK) serial dilutions of the bacterial suspension were made down to a x 10^7 dilution.

Following the Miles and Misra method [21], 3 × 20 µ1 of each dilution was pipetted into a quadrant of a BHI agar plate. The agar plates were carefully transported horizontally and left for approximately 5 min in the incubator (Thermo scientific, HERAcell 150i, CO2 incubator, UK) with their lids slightly open to allow the suspension to dry. The plate lids were then closed, wrapped in clingfilm, labelled, and inoculated at 37 °C, 5 % CO_2 for 24 h for *SA*. For *FN* the same procedure was used but the plates were left in the anaerobic chamber for 24 h or until colonies could be counted. The number of colonies forming units (CFUs) at each dilution was recorded. The number of colonies per ml was then calculated as in the following formula.

CFU per ml = Average number of colonies for a dilution x 50 x dilution factor [21].

2.6. Characterization of materials after bacterial challenge

The changes to the material surface induced by contact with bacteria at each time point were assessed by grazing angle X-ray diffraction analyses using asymmetric Bragg (GIAB) mode. Near-surface analysis was performed using a Rigaku Ultima IV with a CuKa source set in grazing incidence mode with an incidence angle of 3 degrees. The diffractometer was operated at 40 mA and 45 kV from 20 to 70 degrees 2θ range with a sampling width of 0.05 degrees, and a scan speed 0.5 degrees/minute. The specimens were again continuously rotated at 15 revolutions per minute. Phase identification was accomplished using a search match software indexing the peaks against Power Diffraction Files (PDF) data provided by the International Centre for Diffraction Data (ICDD).

2.7. Statistical analysis

Normality was tested using descriptive statistics, plots, and Shapiro Wilko normality test. All data showed non-normal distribution, so non-parametric analysis was adopted. Comparisons between the four study groups were performed using Kruskal Wallis test, followed by multiple pairwise comparisons using Bonferroni adjusted significance level. Significance was set at p value < 0.05. Data were analyzed using IBM SPSS for Windows (Version 26.0, IBM Corp.).

3. Results

3.1. Material characterization

The surface morphology of uncoated titanium control (Fig. 1A) changed considerably after the Au pre-coating and CCT. SEM analysis for Ti-control group showed a smooth surface with regular striae resulting from the surface finishing protocol applied to the discs. For CCTed samples with pre-deposited gold layer, a uniform oxide layer was formed over the surface, and the crystallites on the surface increased with the treatment time (Fig. 1B-D). This was confirmed by EDX analysis in Fig. 2. A denser oxide layer with scattered gold particles was noted in the three CCTed samples with pre-deposited gold layer. The uniformly distributed white particles were present in higher concentration in Au-Ti-3 H and Au-Ti-8 H when compared with the Au-Ti 80 H also confirmed by EDX analysis (Table 2 & Fig. 2).

The cross-sectional images (Fig. 3) showed the thickness and microstructure of the coatings. The thickness of the oxide layer formed on non-coated discs after CCT for 3 h was about 0.6–0.8 µm. However, the thickness of the oxide layer increased considerably for samples with a pre-deposited gold layer. It ranged from 2.3–2.65 µm for Au-Ti-3 H, 3.15- 4.5 µm for Au-Ti-8 H and 6.5–8.4 µm for Au-Ti-80 H. It is noted that the pre-deposited gold accelerated oxide formation. The distribution of gold particles was more obvious in the superficial layer, while a few scattered particles were dispersed in the oxide layer. With a similar amount of gold pre-deposited on Ti discs, the thickness of the oxide layer increased with treatment time and temperature which follow oxidation thermodynamics.

The changes in the phase constituents of titanium control and the samples after CCT are shown in Fig. 4. The control titanium disc showed only titanium peaks. After 3 H treatment at 620 °C (Fig. 4A), the major peaks of α-Ti shifted to a lower angle due to the dissolution of oxygen. However, the oxide was barely discernible on the surface of the sample without a pre-deposited gold layer (uncoated Ti-control) mainly because the oxide film was too thin to be detected by normal Bragg-Brentano XRD. In contrast, clear peaks from titanium oxide in rutile form can be seen from the XRD chart of Au-Ti-3 H showing the catalytic action of Au for the formation of surface oxide layer (Fig. 4B). It is also shown that rutile is the dominate oxide phase and very little anatase could be

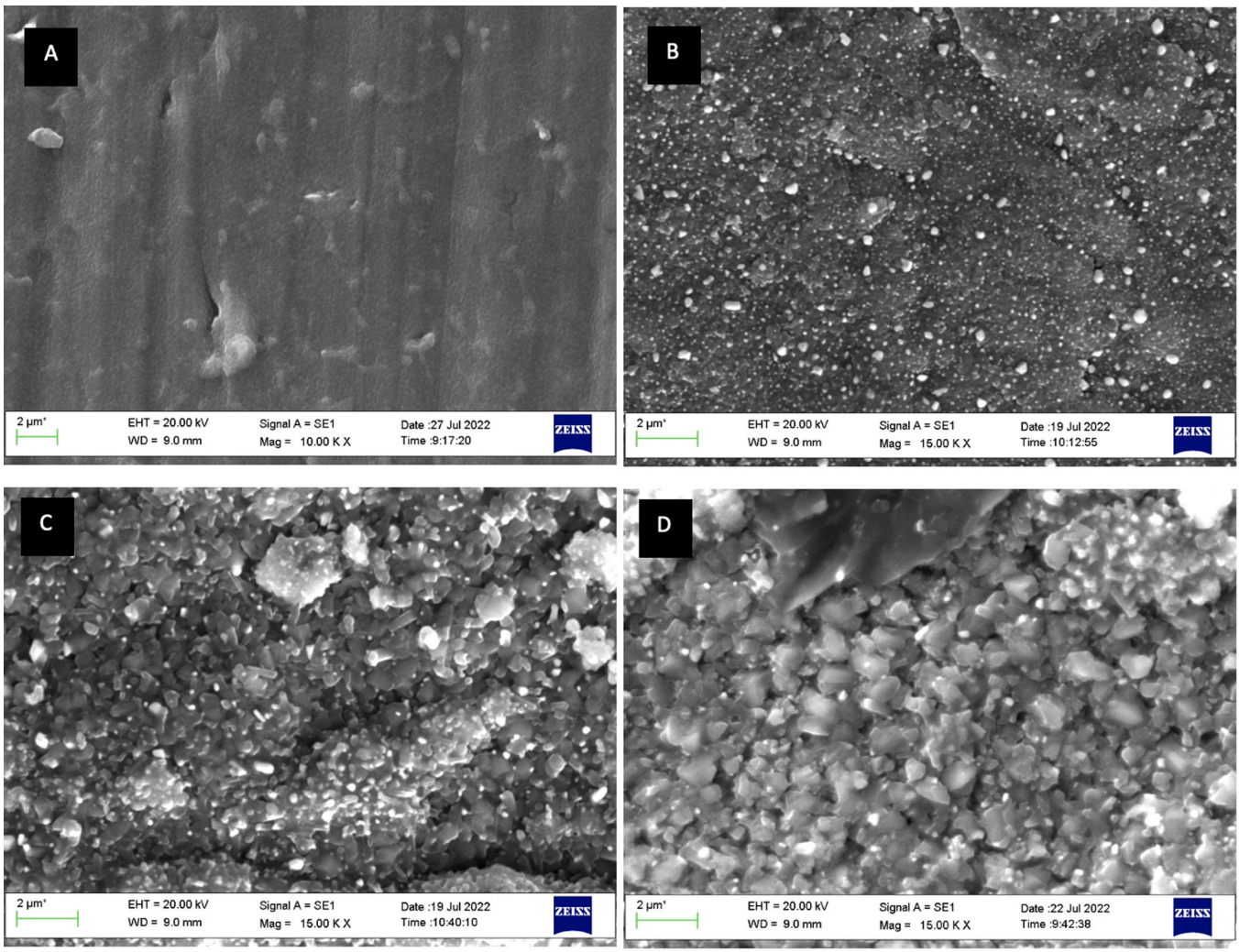

Fig. 1. A-D: Secondary electron scanning electron micrograph of titanium discs showing changes in topography with various treatments. A: control titanium surface (Ti-C) showing a smooth surface with regular striae resulting from the surface finishing protocol applied to discs; B-D: after gold coating and ceramic conversion; B: Au-Ti-3 H, C: Au-Ti-8 H, D: Au-Ti-80 H showing uniform distribution of nano and microparticle coating over the surface of the Ti discs with the gold particles appearing as a white dense particulate deposit. The elemental composition of the particles was verified by EDX analysis.

detected from all CCTed surfaces. Also, gold peaks at low frequency are noted in gold pre-deposited titanium discs (Fig. 4B/C/D).

3.2. Assessment of adhesion of coating

As demonstrated in (Fig. 5A), for the Au-Ti-3 H surfaces, the friction force increased steadily with the load till about 20 N, and it then fluctuated at a higher range corresponding to the large range of change of 1st derivative. There were rarely any chips or flakes formed around the scratch (Fig. 5A) indicating good adhesion of the oxide layer with the substrate. The image of the end of the scratch suggesting the oxide layer was cut through at some point which might be gradual as the force change was not sharp at the load between 15–20 mN. The smaller load indicated that the oxide layer was thinner than Au-Ti-8 H as shown in Fig. 5.

In contrast, flakes of the oxide layer started to be seen at the sides of the scratches for sample Au-Ti-8 H (Fig. 5B) and Au-Ti-80 H (Fig. 5C) when the load increased from 5 to 10 N. The number and size of the chips both increased with the load increase at 30 N as shown in Figs. 5B and 5C. The friction forces are more unstable for both these two samples especially with increased load indicating a less coherent oxide layer for a thick oxide layer formed on Au-Ti-8 H and Au-Ti-80 H. The tested samples did not show any sudden jump in the friction force and least chips and broken parts are noticed in the short-time treated discs Au-Ti-3 H (Fig. 5A) than the other two samples indicating better adhesion to the underlaying titanium discs.

3.3. Assessment of leaching

The leaching profile of the test materials is shown in Table 3. There was no difference in the leaching of titanium or gold over the 28 days period for all coatings compared to the uncoated titanium ($p > 0.05$).

3.4. Direct attachment assay testing

For both bacterial species a statistically significant difference was noted on comparing Ti-C discs to Au-coated Ti-discs with the latter showing a great reduction in the growth of bacterial colonies particularly *FN* as shown in Table 4 with a P-value < 0.001. Adhesion of *SA* to Ti-C discs recorded values of $1601.00 \pm 887.04 \times 10^4$ CFU/ml which was significantly higher than those reported for the CCT treated titanium discs Au-Ti 3 H at $10.28 \pm 8.61 \times 10^4$), Au-Ti 8 H ($166.50 \pm 99.34 \times 10^4$) and Au-Ti 80 H ($85.25 \pm 81.25 \times 10^4$). A similar result was noted for *FN* were Ti-C discs showed higher bacterial adhesion in comparison to the Au CCT titanium discs.

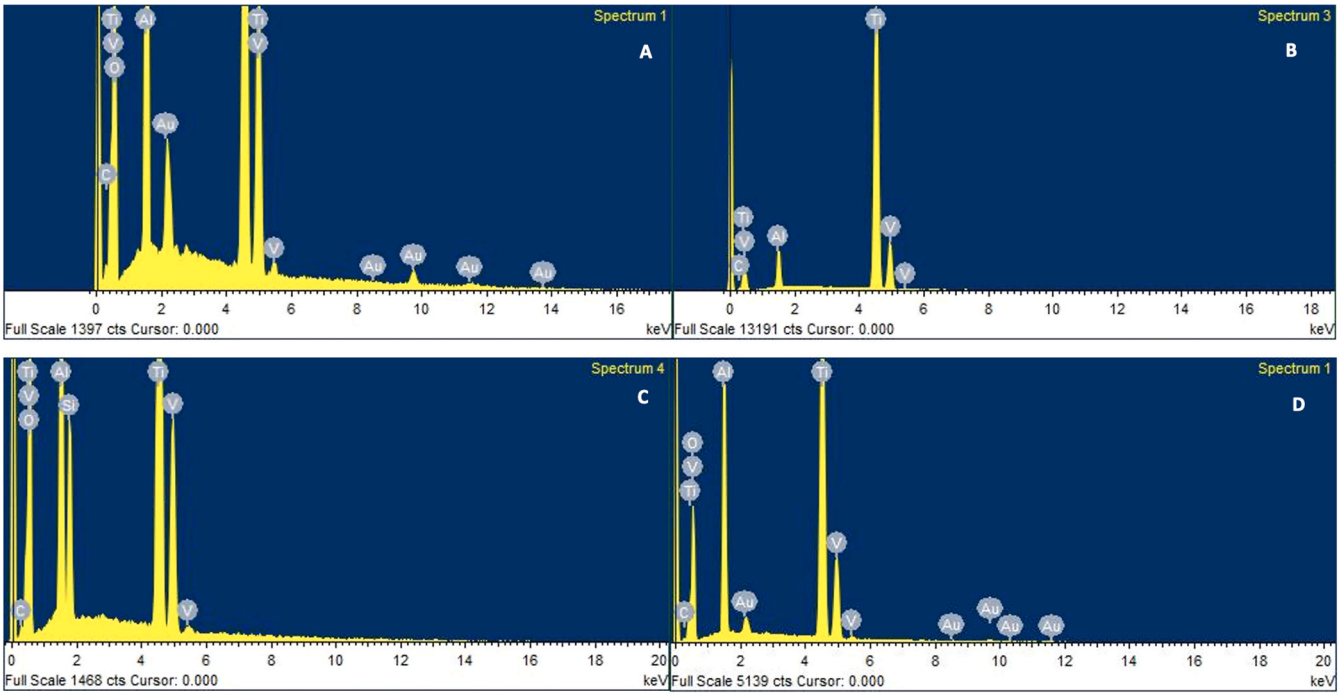

Fig. 2. A: elemental analysis for the Ti-C discs showing the presence of titanium, B: Au-Ti 3 H showing the elemental composition of the surface after CCT of titanium discs demonstrating abundant oxide surface layer and gold which accelerates the oxide layer formation, C: Au-Ti 8 H and D: Au-Ti 80 H.

Table 2
showing different elements composition of the treated titanium discs.

Elements	Ti-control (wt%)	Au-Ti-3 H (wt%)	Au-Ti-8 H (wt%)	Au-Ti-80 H (wt%)
titanium	88.2	42.2	41.52	39.07
gold	-	4.46	4.88	2.44
oxygen	-	41.16	41.26	44.11
aluminium	7.84	8.72	8.82	10.91
vanadium	3.95	3.46	3.52	3.47

3.5. Characterization of materials after bacterial challenge

The surface phase changes before and after the bacterial challenge are shown in Fig. 6. There were no phase changes noted in the control and coated titanium for all ceramic conversion treatments. The 3-hour ceramic conversion coating showed the presence of titanium together with the oxide and gold for both water immersion and after bacterial culture. The titanium was no longer visible with increasing coating thickness for the longer ceramic conversion treatments.

4. Discussion

The current study investigated gold pre-deposited titanium abutments, where a layer of gold/titanium dioxide was produced over the titanium by Au-catalysed ceramic conversion treatment with different treatment protocols to produce a gold-doped titanium dioxide (Au-TiO2) coating. Physical-chemical and adhesion properties of the coating were assessed by SEM/EDX (microstructure & composition), XRD (phase constituents) and scratch analysis (bonding strength). In addition, the leaching of gold and titanium in solution and the antimicrobial properties were assessed together with phase changes after the microbial challenge. The antimicrobial activity of coated discs was tested using direct attachment assays.

Osseo integrated dental implants have become the preferred option for replacing missing teeth, with a very high survival rate, owing to their biocompatibility, corrosion resistance, good tissue response and the presence of the active titanium oxide outer layer. Infection occurring after placement of dental implants represents one of the major complications despite use of aseptic surgical measures [22,23]. The literature indicates that 14 % of implant failures are related to post placement bacterial infections [24].

Peri-implantitis which occurs after implant loading has been associated with the presence of a biofilm rich in *Fusobacterium spp*., *Staphylococcus spp*, *Porphyromonas gingivalis*, and *Aggregatibacter actinomycetemcomitans*. Therefore, this research aimed to examine a novel CCT of gold pre-deposited titanium discs and explore its surface characteristics and antimicrobial properties against bacteria commonly implicated in peri-implant infections.

Gold was utilized in the current study owing to its long-term stability and exceptional frictional characteristics [25]. Furthermore, gold nanoparticles of titanium alloys can enhance its photocatalytic [16,26] and antimicrobial activity which may decrease the rate of peri-implant tissue inflammation. To increase the number of new titanium atoms that react to oxygen, the existence of a gold layer on the surface of the titanium alloy has been promoted, and the outward diffusion of titanium ions has been encouraged to increase the number of new titanium atoms that react to oxygen [15,27].

SEM analysis of tested discs revealed the changes in surface features from a smooth, straited surface to a meshwork with numerous scattered, white particles (Au particles) which confirmed the formation of an oxide layer on the surface and that gold accelerated Ti oxidation progress and formation in a similar manner as previous studies [15,16]. For the surface characterization of the CCT of titanium alloy, more oxide layer formation was detected, as gold accelerates the formation of a thicker oxide layer during increasing the heat treatment from 3 h to 80 h, which is attributed to the increased outward migration of titanium atoms to react with oxygen to form a thicker oxide layer [15,16]. Gold atoms preferentially bind to titanium atoms rather than oxygen, facilitating the formation of a strongly bound oxygen/transition metal system that can enhance its reactivity. The gold clusters in addition to the oxides could possess a high catalytic activity. Oxygen can be mainly adsorbed at the Au-TiO_2 interface increasing its availability for oxidation of Ti, here Au acts as a catalyst accelerating the oxidation process [28,29].

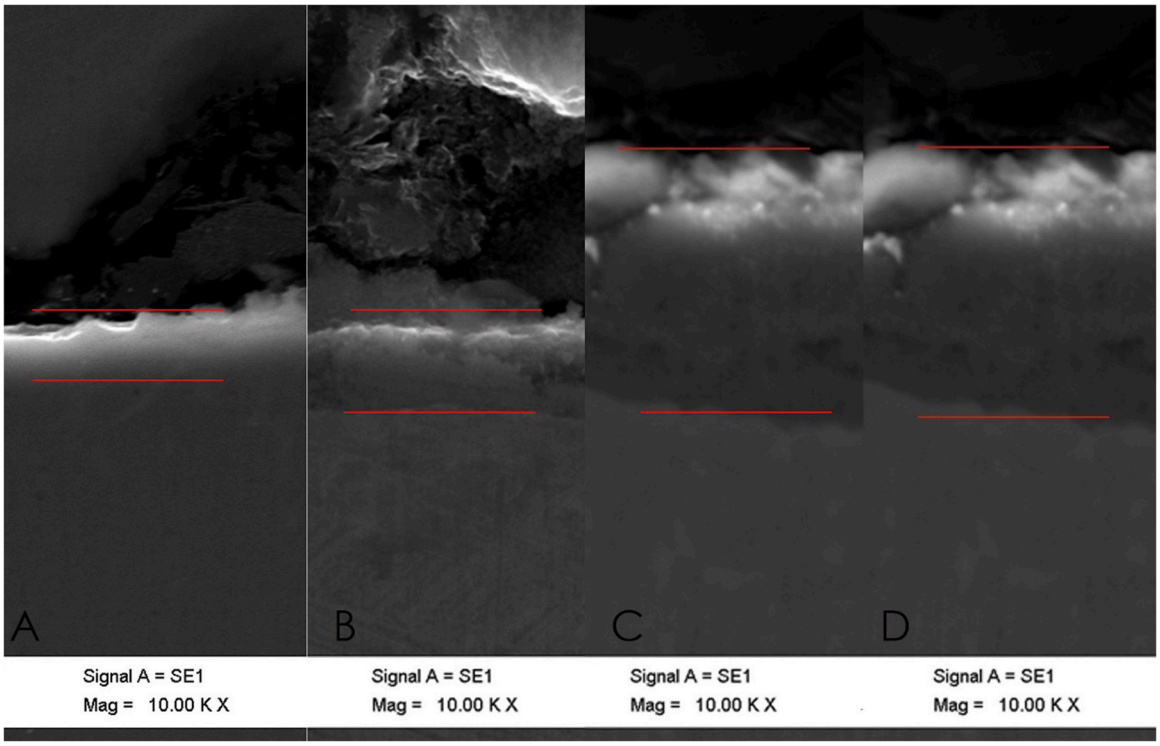

Fig. 3. Cross-sectional secondary electron scanning electron images of control and ceramic conversion treated titanium showing the oxide layer with different thicknesses for the different times of ceramic conversion treatment.

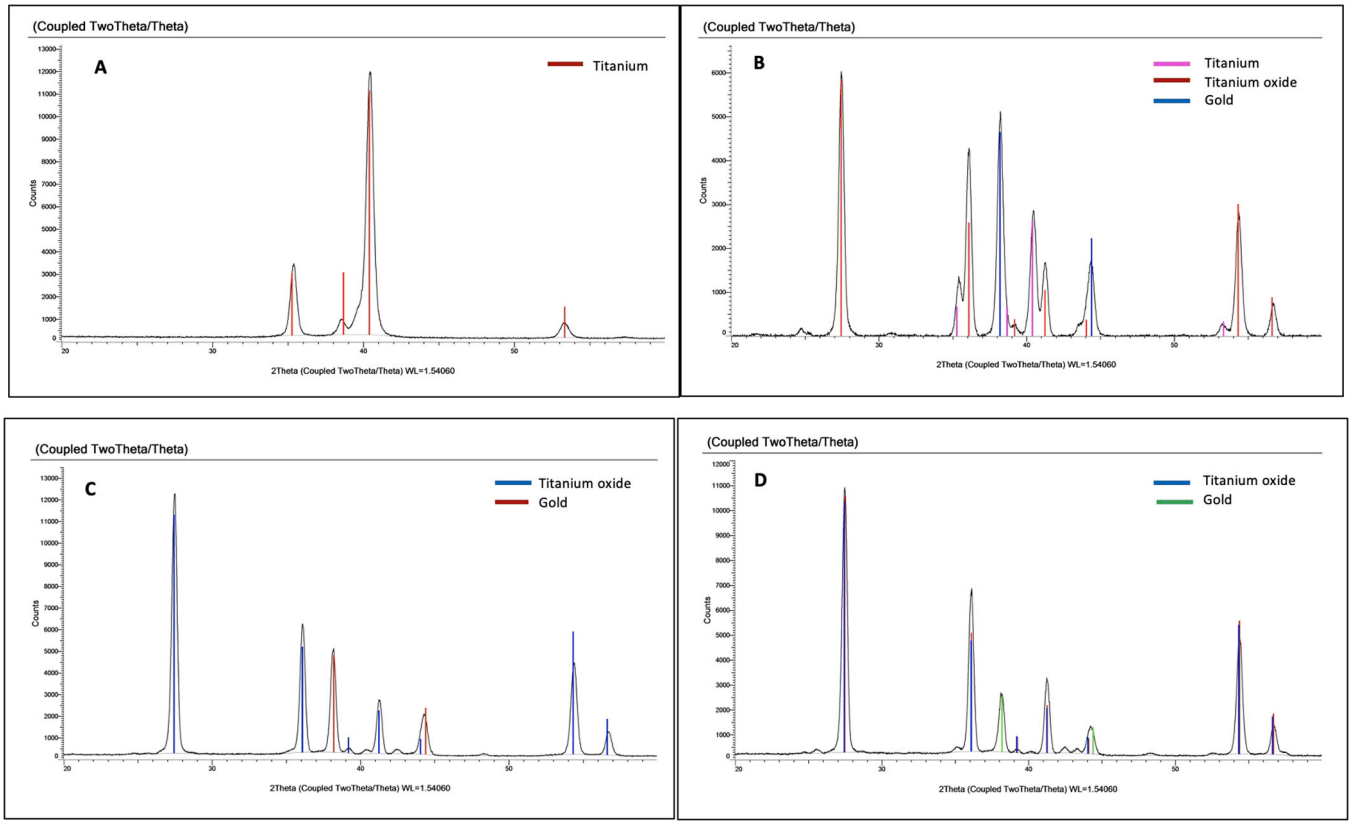

Fig. 4. X-ray diffraction patterns of A: Ti-C discs with only titanium peaks noted, B: Au-Ti 3 H discs showing titanium oxide phase formed together with gold peaks detected, C: Au-Ti 8 H discs demonstrating the more dominant titanium oxide and gold peaks, D: Au-Ti 80 H discs also showing titanium oxide phase and gold peaks.

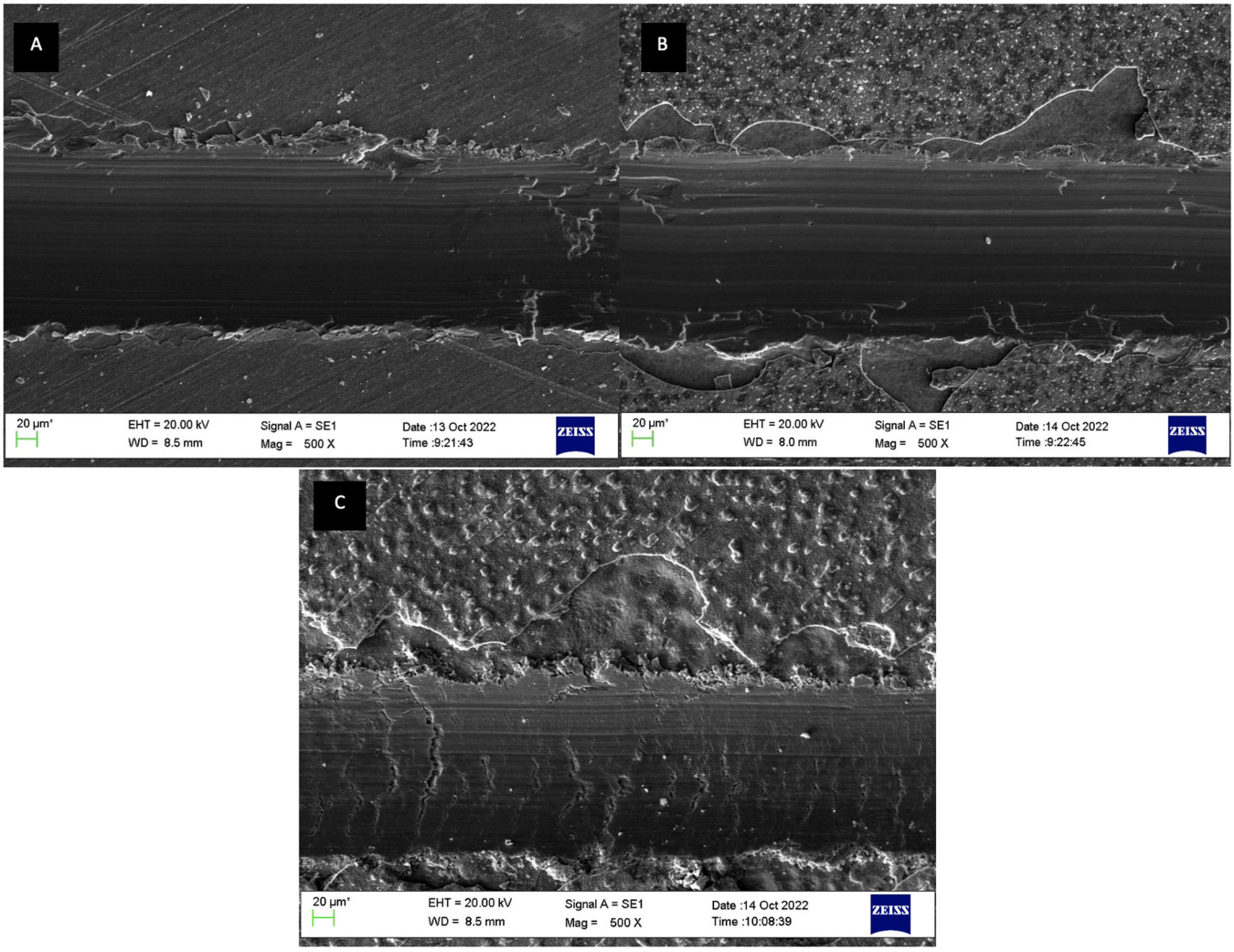

Fig. 5. Scanning electron micrographs of the tested ceramic converted treated titanium after scratch testing, A: Au-Ti-3 H showing better surface adhesion for the coat and less chips and cracks on the periphery, unlike B: Au-Ti-8 H and C: Au-Ti-80 H that showed less coat adhesion and more chips and cracks demonstrated in both figures.

Table 3
Leaching profile of the uncoated and coated titanium discs over a period of 28 days (mean ± SD).

Coating	Elements released mg/l					
	7 days		14 days		28 days	
	Ti	Au	Ti	Au	Ti	Au
Ti-C	BDL	BDL	BDL	BDL	BDL	BDL
Au-Ti-3 H	BDL	95.82 ± 82.75	BDL	5.29 ± 3.37	BDL	BDL
Au-Ti-8 H	BDL	17.03 ± 6.26	BDL	1.25 ± 0.72	BDL	BDL
Au-Ti-80 H	BDL	5.54 ± 3.22	BDL	BDL	BDL	BDL

BDL: below detection limi

The phase changes were monitored by X-ray diffraction analysis which was undertaken on the untreated titanium, after the sputter coating and catalytic conversion and after the antimicrobial testing. The untreated discs showed peaks for titanium whilst peaks for oxides was not detected. After CCT of the titanium discs, clear peaks of rutile oxide were observed, indicating the catalytic effect of Au on the formation of the oxide layer. Rutile has also been demonstrated to be the predominant oxide phase and very little anatase was observed on all CCT treated surfaces. This is consistent with literature which suggests that if titanium or its alloys are exposed to air temperatures of 600 °C or above, the rutile will dominate [30]. With the increase in oxide thickness, a more scattering of gold was noticed and this caused significant decreases to the amount of gold left over at the interface. Therefore, this reduces active role of the Au nanoparticle and thus slows down the oxidation rate after a thick oxide layer formed [31] XRD analysis of the treated discs after both immersion in distilled water and bacterial exposure, showed that no significant change in the phase constituents of the treated discs, with the dominant rutile phase and the presence of some anatase phase in longer treatment cycles, which confirms that immersion of the treated discs did not change the surface chemistry and characteristics. Such findings prove the stability of such coating during function in the oral cavity with minimal interactions involved.

For the scratch test, the tested groups showed a similar adhesion pattern, with a better adhesion related to AU-Ti-3 H. This was because the oxide layer greatly reduced the adhesive action of metal/ceramic contact because of the nature of the ceramic/ceramic contact thus reducing the friction and potentially improving the wear resistance of the materials. Gold particles could self-restore under the applied load because of their low shear strength even if a local failure occurred in the TiO_2 layer, therefore reducing the friction, and increasing the wear resistance in a sliding test [31], also the better adhesion with minimal cracking is due to the thinner oxide thickness in 3 h treated discs. With the presence of the pre-deposited gold, the quality of the oxide layer was

Table 4
Statistical analysis for both tested bacterial species SA & FN showing a statistical significant reduction for Au coated discs in comparison to untreated Ti-C discs.

Bacterial species	Test groups	Mean ± SD	Median (IQR)	P value
FN	Ti-C	$239.00 \pm 40.61 \times 10^4$ **a**	$228.00\ (81.00) \times 10^4$	< 0.001*
	Au-Ti-3 H	$0.004 \pm 0.007 \times 10^4$ **b**	$0.00\ (0.012) \times 10^4$	
	Au-Ti-8 H	$0.049 \pm 0.031 \times 10^4$ **b**	$0.0555\ (0.061) \times 10^4$	
	Au- Ti-80 H	$0.0245 \pm 0.008 \times 10^4$ **b**	$0.0245\ (0.016) \times 10^4$	
SA	Ti-C	$1601.00 \pm 887.04 \times 10^4$ **a**	$1800.00\ (1463.00) \times 10^4$	< 0.001*
	Au-Ti-3 H	$10.28 \pm 8.61 \times 10^4$ **b**	$10.25\ (16.93) \times 10^4$	
	Au-Ti-8 H	$166.50 \pm 99.34 \times 10^4$ **b**	$180.00\ (210.50) \times 10^4$	
	Au-Ti-80 H	$85.25 \pm 81.25 \times 10^4$ **b**	$85.00\ (158.25) \times 10^4$	

SD: Standard Deviation, IQR: Interquartile range
a,b: different letters denote statistically significant differences between groups using Bonferroni adjustment
Units: in CFU/ml
* statistically significant at p value < 0.05

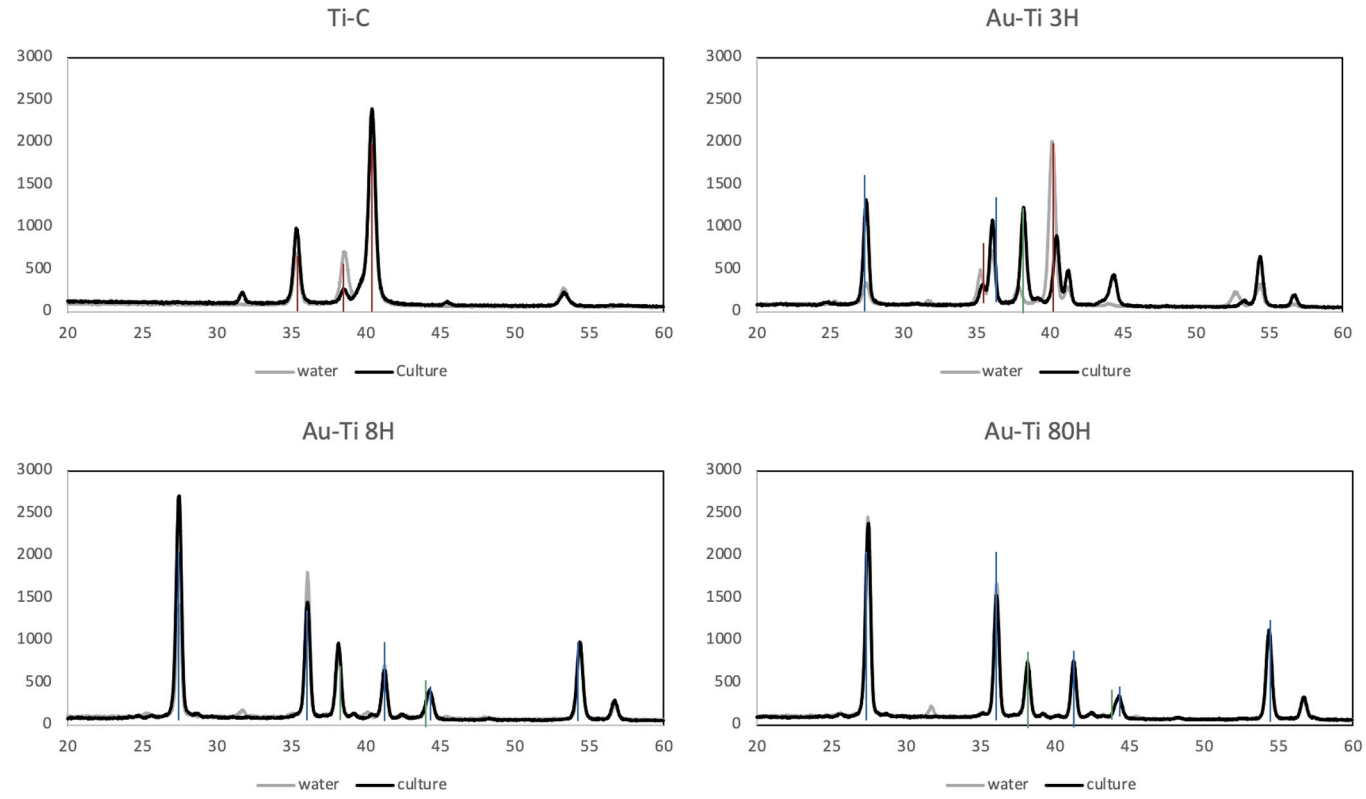

Fig. 6. X-ray diffraction plots of titanium and coated titanium immersed in water and after antimicrobial testing showing no changes to the main peaks observed titanium; titanium oxide; gold.

improved and there was no spallation found in the scratch wear test especially in low coat thicknesses in line with fundings from others [30].

For Au-Ti-8 H and Au-Ti-80 H, the scratch test tracks were deeper and wider with higher fluctuations in the load applied. Also, parts of the oxide layers were peeled off owing to an increase in the oxide layer thickness 5 μm or more. Further cracks in the oxide layer, which led to partial spallation on the scratch and wear test, were formed because of the increased thickness and defects in the oxide layer as shown in Fig. 3C/D [32].

To evenly cover the titanium discs, the sputtering technique which has been successfully applied to produce thin material films on surfaces was employed. The AuNPs added to the surface may retain their antimicrobial qualities [33]. Gold was released from Au-Ti-3 H coated discs into water suggesting the coating did not hinder release of gold and its antimicrobial properties. No correlations between the coating and the antimicrobial properties could be made due to the large standard deviation obtained. For the anti-microbial properties of Au treated discs, there was a statistically significant reduction in the bacterial count compared to untreated titanium discs. These findings support the antimicrobial effect of gold particles that leads to a significant reduction in bacterial count of both *SA* and *FN*. This finding agreed with previous research [34] suggesting that when Au ions come into contact with the bacteria cell, they are usually dispersed within the bacterial micro-environment without a specific location. On the other hand, a focused source of Au that can constantly release ions like gold nanoparticles which are interconnected to the bacterial cell walls can increase toxicity in cells resulting in accelerated bacterial cell death.

Significant lower bacterial counts were noted in the anaerobic, Gram-negative bacterial species (*FN*) in comparison to the aerobic, Gram positive species (*SA*) in all the tested groups which has already been reported [35]. That may be due to the fact that Gram positive bacteria have a thick cell wall, whereas Gram negative bacteria have an outer membrane and a thin peptidoglycan layer which may allow Au nanoparticles to penetrate through the membrane and cause cellular damage [36]. The antimicrobial properties of Au nanoparticles are reported to achieve antimicrobial actions by two processes. Firstly,

altering the membrane potential and reducing ATP synthase activity of adenosine triphosphate, these inhibitors inhibited metabolic processes. Secondly, ribosome subunits for tRNA binding have been rejected to effectively destroy its biological process [36].

Important aspects are the concentration and size of the nanoparticles, which play a vital role in the antimicrobial mechanism. The antimicrobial properties of Au nanoparticles on Gram positive and Gram negative bacteria depends on the concentration of the gold in the coating [37,38]. It was demonstrated that the catalytic and antimicrobial efficacy of the Au nanoparticles increases with higher concentration, shown by Au-Ti-3 H having the highest antimicrobial effect most likely due to the higher gold percentage and smaller particle size found in the oxide layer as confirmed by SEM/EDX analysis (Fig. 1B/Fig. 2B).

5. Conclusions

The findings in the current study showed that the presence of a thin gold layer promoted the formation and acceleration of oxide layer formation over titanium grade V discs. A uniform adherent coating was formed after ceramic conversion treatment of titanium. Better adherence and uniformity were noted in the thin oxide layer formed with a 3-hour ceramic conversion treatment in comparison to thicker layers (8 and 80 h) in longer treatment periods. The coated titanium exhibited antimicrobial properties. The results of this study suggest the potential use for coated implants in managing plaque biofilm and reducing the incidence of plaque related peri-implant diseases.

6. Recommendations

More elaborative research on the toxic effect of gold nanoparticles on the human cells as well as examining its effect on eukaryotic cells.

Acknowledgements

Thanks to the Ministry of higher education and scientific research (Egypt)b for funding Dr. Yasser Mohamed Aly during his stay in Birmingham university to accomplish this research.

References

[1] AlQahtani SM. Awareness and acceptance of dental implants as a treatment modality for replacement of missing teeth among patients in Aseer region Kingdom of Saudi Arabia. Int J Oral Care Res 2018;6(1):58–64.
[2] Arora JrK, Kaur IIN, Kaur IIIG, Garg IVU, Kaur N, Kaur G, et al. Knowledge, awareness, and attitude in using dental implants as an option in replacing missing teeth among dental patients: survey-based research in a dental teaching hospital in Derabassi, Punjab. Cureus 2022;14(7).
[3] Block MS. Dental implants: the last 100 years. J Oral Maxillofac Surg 2018;76(1):11–26.
[4] Buser D, Sennerby L, De Bruyn H. Modern implant dentistry based on osseointegration: 50 years of progress, current trends and open questions. Periodontol 2000 2017;73(1):7–21.
[5] Oshida Y. The 2nd Symposium International of Advanced Bio-Materials. Montreal, Canada. 2000;5–10.
[6] Jennes ME, Naumann M, Peroz S, Beuer F, Schmidt F. Antibacterial effects of modified implant abutment surfaces for the prevention of peri-implantitis—a systematic review. Antibiotics 2021;10(11):1350.
[7] Derks J, Tomasi C. Peri-implant health and disease. A systematic review of current epidemiology. J Clin Periodo 2015;42(S16):S158–71. Apr 1.
[8] Smeets R, Henningsen A, Jung O, Heiland M, Hammächer C, Stein JM. Definition, etiology, prevention and treatment of peri-implantitis – a review. Head Face Med 2014;10(1):34.
[9] Dixon DR, London RM. Restorative design and associated risks for peri-implant diseases. Periodontol 2000 2019;81(1):167–78.
[10] Mahn DH. Implant abutment and restoration design and risk factors for peri-implant disease. Compend Contin Educ Dent 2019;15488578(9):40.
[11] Zandim-Barcelos DL, Carvalho GG de, Sapata VM, Villar CC, Hämmerle C, Romito GA. Implant-based factor as possible risk for peri-implantitis. Braz Oral Res 2019;33.
[12] Monje A, Kan JY, Borgnakke W. Impact of local predisposing/precipitating factors and systemic drivers on peri-implant diseases. Clin Implant Dent Relat Res 2023;25(4):640–60.
[13] Göthberg C, Gröndahl K, Omar O, Thomsen P, Slotte C. Bone and soft tissue outcomes, risk factors, and complications of implant-supported prostheses: 5-Years RCT with different abutment types and loading protocols. Clin Implant Dent Relat Res 2018;20(3):313–21.
[14] Shahramian K, Leminen H, Meretoja V, Linderbäck P, Kangasniemi I, Lassila L, et al. Sol–gel derived bioactive coating on zirconia: effect on flexural strength and cell proliferation. J Biomed Mater Res B Appl Biomater 2017;105(8):2401–7. Nov 1.
[15] Zhang Z, Zhang Y, Li X, Alexander J, Dong H. An enhanced ceramic conversion treatment of Ti6Al4V alloy surface by a pre-deposited thin gold layer. J Alloy Compd 2020;844:155867.
[16] Zhang Z, Yu H, Li X, Dong H. Impact of the amount of the gold layer on the tribological performance of the ceramic conversion treated CP-titanium. Tribol Lett 2023;71(2):36.
[17] Martinez A, Guitian F, López-Píriz R, Bartolome JF, Cabal B, Esteban-Tejeda L, et al. Bone loss at implant with titanium abutments coated by soda lime glass containing silver nanoparticles: a histological study in the dog. PLoS One 2014;9(1):e86926.
[18] Littuma GJS, Sordi MB, Borges Curtarelli R, Aragonês Á, da Cruz ACC, Magini RS. Titanium coated with poly(lactic-co-glycolic) acid incorporating simvastatin: Biofunctionalization of dental prosthetic abutments. J Periodontal Res 2020;55(1):116–24.
[19] Qian W, Qiu J, Liu X. Minocycline hydrochloride-loaded graphene oxide films on implant abutments for peri-implantitis treatment in beagle dogs. J Periodo 2020;91(6):792–9.
[20] Colino CI, Lanao JM, Gutierrez-Millan C. Recent advances in functionalized nanomaterials for the diagnosis and treatment of bacterial infections. Mater Sci Eng: C 2021;121:111843.
[21] Miles AA, Misra SS, Irwin JO. The estimation of the bactericidal power of the blood. Epidemiol Infect 1938;38(6):732–49.
[22] Kulkarni Aranya A, Pushalkar S, Zhao M, LeGeros RZ, Zhang Y, Saxena D. Antibacterial and bioactive coatings on titanium implant surfaces. J Biomed Mater Res A 2017 Aug 1;105(8):2218–27.
[23] Dewi RI, Muhammad R, Chiquita P. Titanium implant coating and their effect on osseointegration. AIP Conference Proceedings. AIP Publishing; 2020.
[24] Norowski JrPA, Bumgardner JD. Biomaterial and antibiotic strategies for peri-implantitis: a review (Available from:) J Biomed Mater Res B Appl Biomater 2009;88B(2):530–43. https://doi.org/10.1002/jbm.b.31152.
[25] Antler M, Spalvins T. Lubrication with thin gold films. Gold Bull 1988;21:59–68.
[26] Chen Y, Tang Y, Luo S, Liu C, Li Y. TiO2 nanotube arrays co-loaded with Au nanoparticles and reduced graphene oxide: facile synthesis and promising photocatalytic application. J Alloy Compd 2013;578:242–8.
[27] Kofstad P. High-temperature oxidation of titanium. Journal of the Less Common Metals [Internet]. 1967;12(6):449–464. Available from: ⟨https://www.sciencedirect.com/science/article/pii/0022508867900173⟩.
[28] Hutchings GJ. Selective oxidation using supported gold bimetallic and trimetallic nanoparticles. Catal Today 2014;238:69–73.
[29] Chen MS, Goodman DW. The structure of catalytically active gold on titania. Science (1979) 2004;306(5694):252–5.
[30] Dong H, Bell T. Enhanced wear resistance of titanium surfaces by a new thermal oxidation treatment. Wear 2000;238(2):131–7.
[31] Busiakiewicz A, Kisielewska A, Piwoński I, Batory D, Pabianek K. Formation of gold and platinum nanostructures on rutile TiO2 (001) by thermal treatment of thin films in vacuum. Vacuum 2019;163:248–54.
[32] Abreu CS, Matos J, Cavaleiro A, Alves E, Barradas NP, Vaz F, et al. Tribological characterization of TiO2/Au decorative thin films obtained by PVD magnetron sputtering technology. Wear 2015;330–331:419–28.
[33] Villa-García LD, Márquez-Preciado R, Ortiz-Magdaleno M, Patrón-Soberano OA, Álvarez-Pérez MA, Pozos-Guillén A, et al. Antimicrobial effect of gold nanoparticles in the formation of the Staphylococcus aureus biofilm on a polyethylene surface. Braz J Microbiol 2021;52(2):619–25.
[34] Katas H, Lim CS, Azlan AYHN, Buang F, Busra MFM. Antibacterial activity of biosynthesized gold nanoparticles using biomolecules from Lignosus rhinocerotis and chitosan. Saudi Pharm J 2019;27(2):283–92.
[35] Sathiyaraj S, Suriyakala G, Gandhi AD, Babujanarthanam R, Almaary KS, Chen TW, et al. Biosynthesis, characterization, and antibacterial activity of gold nanoparticles. J Infect Public Health 2021;14(12):1842–7.
[36] Anju VT, Paramanantham P, Sharan SBSL, Syed A, Bahkali NA A, et al. Antimicrobial photodynamic activity of toluidine blue-carbon nanotube conjugate against Pseudomonas aeruginosa and Staphylococcus aureus-understanding the mechanism of action. Photo Photo Ther 2019;27:305–16.
[37] Belliraj TS, Nanda A, Ragunathan R. In-vitro hepatoprotective activity of Moringa oleifera mediated synthesis of gold nanoparticles. J Chem Pharm Res 2015;7(2):781–8.
[38] Lin C, Tao K, Hua D, Ma Z, Zhou S. Size effect of gold nanoparticles in catalytic reduction of p-nitrophenol with NaBH4. Molecules 2013;18(10):12609–20.